	vitro,				
Y. Harada, T. Yamamoto, M. Sakai, T. Saiki, K. Kawano, Y. Maitani and M. Yokoyama	Effects of organic solvents on drug incorporation into polymeric carriers and morphological analyses of drug-incorporated polymeric micelles.	*Int J Pharm.*	404(1-2)	271-280	2011
T. Izumisawa, Y. Hattori, M. Date, K. Toma, Y. Maitani	Cell line-dependent internalization pathways determine DNA transfection efficiency of decaarginine-PEG-lipid.	*Int J Pharm*	404	264–270	2011
Kawano, Y. Maitani	Tumor permeability of nanocarriers observed by dynamic contrast-enhanced magnetic resonance imaging.	*Yakugaku Zasshi*	130(12)	1679-1685	2010
K. Shiraishi, K. Kawano, Y. Maitani, Yokoyama M.	Polyion complex micelle MRI contrast agents from poly(ethylene glycol)-β-poly(l-lysine) block copolymers having Gd-DOTA; preparations and their control of T(1)-relaxivities and blood circulation characteristics.	*J Control Release*	148	160-167	2010
Y. Hattori, N. Kanamoto, K. Kawano, H. Iwakura, M. Sone, M.Miura, A. Yasoda, N. Tamura, H. Arai, T. Akamizu, K. Nakao, Y. Maitani	Molecular characterization of tumors from a transgenic mice adrenal tumor model: Comparison with human	*International Journal of Oncology*	37	695-705	2010

	pheochromocytoma.				
Y. Taniguchi, K. Kawano, T. Minowa, T. Sugino, Y. Shimojo, Y. Maitani	Enhanced Antitumor Efficacy of Folate-linked Liposomal Doxorubicin with TGF-β Type I Receptor Inhibitor.	*Cancer Science*	101	2207-2213	2010
A. Hioki, A. Wakasugi, K. Kawano, Y. Hattori, Y. Maitani	Development of an In Vitro Drug Release Assay of PEGylated Liposome Using Bovine Serum Albumin and High Temperature.	*Biol. Pharm. Bull*	33	1466-1470	2010
Y. Maitani	Lipoplex formation using liposomes prepared by ethanol injection.	*Methods Mol Biol*	605	393-403	2010
Y. Hattori, M. Hakoshima, K. Koga and Y. Maitani	Increase of therapeutic effect by treating nasopharyngeal tumor with combination of HER-2 siRNA and paclitaxel.	*International Journal of Oncology*	36	1039-1046	2010
K. Koga , Y. Hattori, M. Komori, R. Narishima, M. Yamasaki, M. Hakoshima, T. Fukui and Y. Maitani	Combination of RET siRNA and irinotecan inhibited the growth of medullary thyroid carcinoma TT cells and xenografts via apoptosis.	*Cancer Science*	101	941-947	2010
H. Ma, K. Shiraishi, T. Minowa, K. Kawano, M. Yokoyama, Y. Hattori, Y. Maitani	Accelerated blood clearance was not induced for a gadolinium-containing PEG-poly(L-lysine)-based polymeric micelle in mice.	*Pharm. Res.*	27(2)	296-302	2010

研究成果の刊行物・別刷

13 Molecular Mobility of Freeze-Dried Formulations as Determined by NMR Relaxation Times, and Its Effect on Storage Stability

Sumie Yoshioka
University of Connecticut, Storrs, Connecticut, U.S.A.

Yukio Aso
National Institute of Health Sciences, Tokyo, Japan

INTRODUCTION

Freeze-drying is a useful method for preparing dosage forms of thermally unstable pharmaceuticals without the deleterious effect of heat. The method can also provide a dry product of pharmaceuticals with longer shelf life than solutions or suspensions. Although glassy-state formulations obtained by freeze-drying generally exhibit sufficient storage stability for pharmaceuticals, degradation during storage has been observed in various freeze-dried formulations.

Many studies have demonstrated that storage stability of freeze-dried formulations is related to molecular mobility (1–15). Chemical and physical degradation of small molecules and proteins is enhanced by an increase in molecular mobility associated with moisture sorption. Additives that decrease the molecular mobility of formulations are often effective for the stabilization of the formulation.

This chapter describes molecular mobility of freeze-dried formulations as determined by NMR relaxation times and discusses the relationship between storage stability and NMR-determined molecular mobility.

MOLECULAR MOBILITY AS DETERMINED BY NMR RELAXATION TIMES

NMR has been used to determine molecular mobility of freeze-dried formulations (16–20), along with other techniques like calorimetry, dielectric relaxation spectrometry, and dynamic mechanical measurement (21–25). NMR can determine the mobility of atoms in pharmaceutical molecules such as ^{1}H, ^{2}H, ^{13}C, ^{15}N, ^{17}O, and ^{19}F. To determine the mobility of a specific site in the molecule, high-resolution solid-state NMR with high sensitivity is necessary. Especially, high sensitivity is inevitable for ^{13}C and ^{15}N, which have low natural abundance. In contrast, low-frequency solid-state NMR, which is easier to operate than high-resolution NMR, can be used to determine the mobility of ^{1}H and ^{19}F, which have high natural abundance. This section addresses the molecular mobility of ^{1}H, ^{13}C, and ^{19}F measured by each of low-frequency solid-state NMR and high-resolution solid-state NMR.

Molecular Mobility as Determined by Low-Frequency NMR

Spin-Spin Relaxation Time of Proton

Spin-spin relaxation time (T_2) of protons present in freeze-dried formulations can be determined from free induction decay (FID). Figure 1 shows the FID of

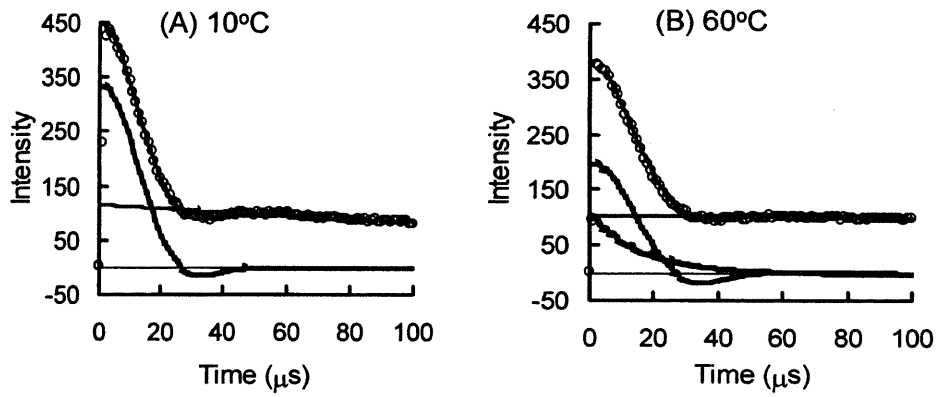

FIGURE 1 Free induction decay of proton in freeze-dried γ-globulin formulation containing dextran at 10°C (**A**) and 60°C (**B**) at 60% RH. *Abbreviation*: RH, relative humidity.

proton in freeze-dried formulation containing γ-globulin as a model protein drug and dextran (molecular weight of 10 kDa) as a polymer excipient, measured by a low-frequency NMR using "solid echo" in the detection stage (26). The FID shows two relaxation processes at 10°C and 60% relative humidity (RH) (Fig. 1A); a slower decay described by the Lorentzian equation (equation 1) and a faster decay described by a Gaussian-type equation (the Abragam equation, equation 2 with a constant c of 0.12). This slower decay is attributed to protons with higher mobility, that is, water protons, and the faster decay is attributed to protons with lower mobility, that is, protons of γ-globulin and dextran. The contribution of protein protons to the FID is not significant because the content of protein was 50 times less than that of dextran. Therefore, the Abragam decay can be considered to be due to dextran protons. The observed FID is describable by an equation representing the sum of the Abragam and Lorentzian equations (equation 3). The T_2 of water protons can be calculated from the FID signals at the latter stage. Subsequently, the T_2 of dextran proton with lower mobility can be calculated from the FID signals at the former stage by inserting the calculated T_2 of water proton into equation (3).

$$F(t) = A\exp\left(-\frac{t}{T_{2(\mathrm{hm})}}\right) \tag{1}$$

$$F(t) = A\exp\left(-\frac{t^2}{2T_{2(\mathrm{lm})}{}^2}\right)\frac{\sin(ct)}{ct} \tag{2}$$

$$F(t) = (1 - P_{\mathrm{hm}})\exp\left(-\frac{t^2}{2T_{2(\mathrm{lm})}{}^2}\right)\frac{\sin(ct)}{ct} + P_{\mathrm{hm}}\exp\left(-\frac{t}{T_{2(\mathrm{hm})}}\right) \tag{3}$$

where $T_{2(\mathrm{hm})}$ and $T_{2(\mathrm{lm})}$ are the spin-spin relaxation times of protons with higher mobility and lower mobility, respectively. P_{hm} is the proportion of protons with higher mobility.

As shown in Figure 1B, the decay due to dextran protons at 60°C cannot be described by a single Abragam equation, and therefore requires further solving by the Lorentzian equation. This indicates that at 60°C, the dextran protons in the freeze-dried formulation exhibit a slower relaxation process due to higher mobility in addition to a faster relaxation process due to lower mobility. In other words, dextran protons having higher mobility exist in the formulation at 60°C, in addition to solid-like dextran protons with lower mobility. Thus, the FID at 60°C is described by an equation representing the sum of the Abragam and Lorentzian equations for dextran protons as well as the Lorentzian equation for water protons. The proportion of dextran protons having higher mobility can be calculated by fitting FID signals into equation (3) after subtracting signals due to water protons.

The temperature at which the spin-spin relaxation of proton begins to involve the Lorentzian relaxation process due to polymer protons having higher mobility in addition to the Gaussian-type relaxation process due to polymer protons having low mobility is considered to be a glass/rubber transition temperature. Basically, this is a critical temperature of molecular mobility as determined by NMR relaxation measurements and is analogous to glass transition temperature (T_g) determined by differential scanning calorimetry (DSC). This critical mobility temperature is referred to as T_{mc}. The T_{mc} of formulations containing polymer excipients increases as the molecular weight of the polymers increases. The T_{mc} of a formulation containing dextran with a molecular weight of 510 kDa is 5°C higher than that for dextran with a molecular weight of 40 kDa. Similarly, the T_{mc} of molecular weight 120 kDa poly(vinyl alcohol) (PVA) formulation is approximately 5°C higher than that of molecular weight 18 kDa PVA formulation (27). In contrast, the T_2 of water proton calculated by the Lorentzian equation is not significantly affected by the molecular weight of dextran (26). This indicates that the mobility of water molecules in the formulation is determined by the interaction between the glucose unit and water.

Figure 2 shows the effect of water content on the T_{mc} and T_g of freeze-dried γ-globulin formulations containing dextran, polyvinylpyrrolidone (PVP) and α,β-poly(*N*-hydroxyethyl)-L-aspartamide (PHEA) (28). T_{mc} shifts to a lower temperature as water content increases, indicating that the molecular

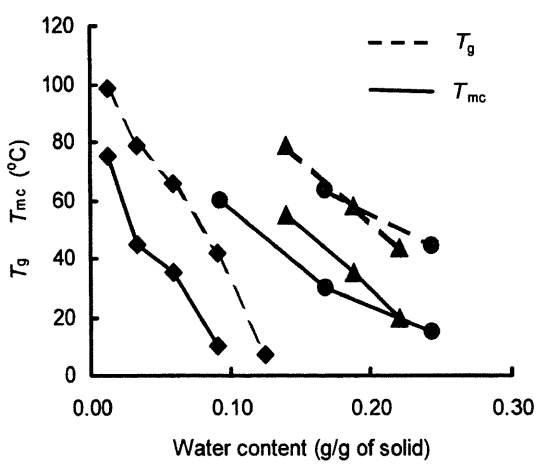

FIGURE 2 T_{mc} and glass transition temperature of freeze-dried γ-globulin formulations containing PHEA (■), dextran (▲), and PVP (●). *Abbreviations*: PHEA, α,β-poly (*N*-hydroxyethyl)-L-aspartamide; PVP, polyvinylpyrrolidone.

mobility of polymer excipients in the formulation is increased by the plasticizing effect of water. Decrease in T_{mc} with increasing water content is also observed for other freeze-dried formulations containing PVA, methylcellulose (MC), hydroxypropylmethylcellulose, and carboxymethylcellulose sodium salt.

The T_{mc} of freeze-dried formulations containing polymer excipients is generally observed at a temperature of 20°C to 30°C lower than the T_g determined by DSC (Fig. 2). This indicates that these formulations have highly mobile protons even at temperatures below the T_g. T_{mc} can be considered to be the temperature at which a certain region of the molecule, such as terminal units of polymer chains, begins to have greater mobility. T_{mc} is a glass/rubber transition temperature determined by spin-spin relaxation measurements, which can detect local changes in molecular mobility more sensitively than T_g determined by DSC. The T_g of freeze-dried formulations containing polymer excipients with moisture is often difficult to determine because a change in heat capacity at T_g may be overlapped by the peaks of water evaporation and accompanying relaxation processes. Furthermore, certain formulations, especially freeze-dried protein formulations, reveal unclear changes in heat capacity, causing a difficulty in determination of T_g. In such cases, T_{mc} determined by spin-spin relaxation measurement can be a useful measure of T_g.

Laboratory and Rotating Frame Spin-Lattice Relaxation Times of Proton

Along with T_2, spin-lattice relaxation times in laboratory and rotating frames (T_1 and $T_{1\rho}$) can also be used to measure the molecular mobility of freeze-dried formulations. The T_1 and $T_{1\rho}$ of proton reflect the correlation time (τ_c) of the rotational motion of proton. The relationship between τ_c and T_1 can be described as follows:

$$\frac{1}{T_1} = \frac{3}{10}\gamma^4\left(\frac{h}{2\pi}\right)^2 r^{-6}\left(\frac{\tau_c}{1+\omega_0^2\tau_c^2} + \frac{4\tau_c}{1+4\omega_0^2\tau_c^2}\right) \tag{4}$$

where γ is the gyromagnetic ratio of ^1H, h is Planck's constant, ω_0 is the ^1H resonance frequencies, and r is the H-H distance. In contrast, $T_{1\rho}$ can be related to τ_c according to equation (5).

$$\frac{1}{T_{1\rho}} = \frac{A\tau_c}{1+4\omega_1^2\tau_c^2} \tag{5}$$

where ω_1 is the frequency of precession generated by the spin locking field and A is a constant.

Figure 3 shows the relationship between τ_c and T_1 (or $T_{1\rho}$) of proton. When τ_c exhibits an Arrhenius behavior, T_1 (or $T_{1\rho}$) exhibits a similar V-shaped pattern with a minimum as a function of temperature. In the temperature range below the minimum (slow motional regime), T_1 (or $T_{1\rho}$) increases in a linear fashion with decreasing temperature (i.e., with decreasing mobility). In the temperature range above the minimum (fast motional regime), in contrast, T_1 (or $T_{1\rho}$) decreases with decreasing mobility associated with decreasing temperature. T_1 minimum is observed at a higher temperature than $T_{1\rho}$ minimum, such that T_1 sensitively reflects faster motion than $T_{1\rho}$ does.

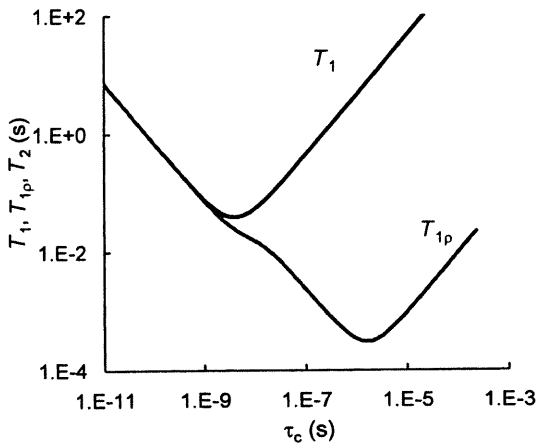

FIGURE 3 Relationship between NMR relaxation times and correlation time.

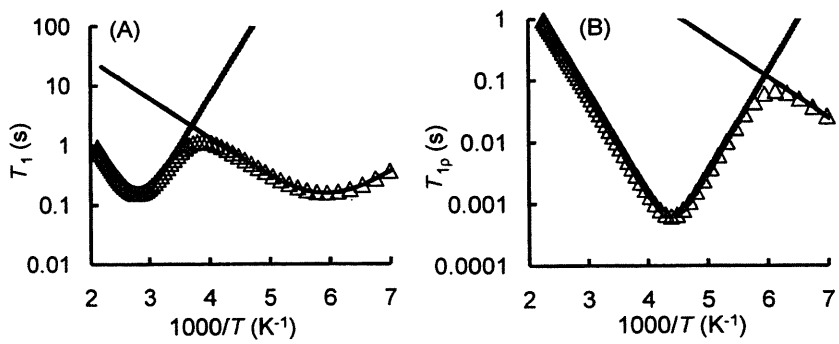

FIGURE 4 Temperature dependence of T_1 (**A**) and $T_{1\rho}$ (**B**) of proton with two correlation times.

When there are multiple protons having different τ_c values in the molecule, spin diffusion occurs between protons located within a short distance, and gives a single T_1 (or $T_{1\rho}$) value. Therefore, the value of T_1 (or $T_{1\rho}$) is determined mainly by a proton that shows the shortest relaxation time. As described by equation (6), relaxation rate (the reciprocal of T_1 and $T_{1\rho}$) can be calculated as the sum of the relaxation rates attributed to each τ_c, when there are two protons having different τ_c values (τ_{c1} and τ_{c2}) in the system. Thus, the observed values of T_1 and $T_{1\rho}$ closely approximate the smaller relaxation times of the two loci, as shown in Figure 4.

$$\frac{1}{T_{1(\text{obs})}} = \frac{P_1}{T_{1(\tau_{c1})}} + \frac{(1-P_1)}{T_{1(\tau_{c2})}} \tag{6}$$

where P_1 is the fraction of proton having τ_{c1}.

Figure 5 shows the temperature dependence of $T_{1\rho}$ observed for freeze-dried γ-globulin formulations containing dextran, prepared using D_2O (29). Since the ratio of γ-globulin to dextran is 1:50, the calculated $T_{1\rho}$ represents the $T_{1\rho}$ of unexchangeable protons of dextran (5 methine protons and 2 methylene protons in a repeating unit). The temperature dependence of $T_{1\rho}$ exhibits a

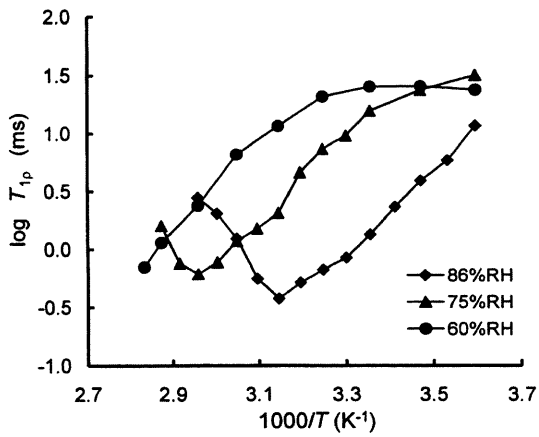

FIGURE 5 Spin-lattice relaxation time of dextran proton in freeze-dried γ-globulin containing dextran.

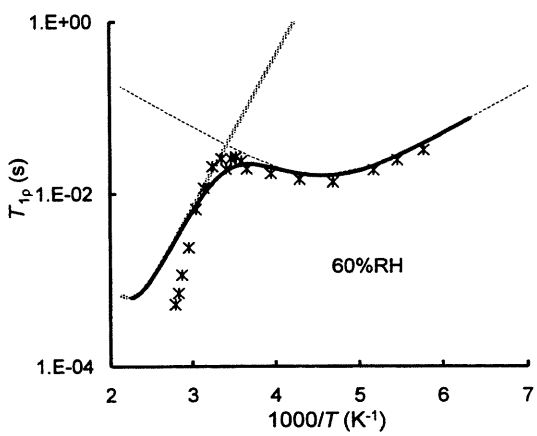

FIGURE 6 Spin-lattice relaxation time of dextran proton in freeze-dried γ-globulin containing dextran in a wider temperature range.

minimum at relatively high humidities (75% and 86% RH). The temperature of the $T_{1\rho}$ minimum shifts to higher temperature as humidity decreases. At 60% RH, minimum is not observed in the temperature range up to 80°C (it may be observed around 90°C), but another minimum is observed at approximately −60°C, as shown in Figure 6. This minimum shifts to approximately 90°C in the dry state. These findings indicate that proton has two different correlation times due to different motions.

The temperature dependence for the $T_{1\rho}$ of proton observed at 60% RH (Fig. 6) can be described by two correlation times (τ_{c1} and τ_{c2}) with an activation energy of 8.0 and 2.5 kcal/mol, and with a pre-exponential factor of 2×10^{-10} and 5×10^{-9}seconds, respectively, at temperatures lower than 35°C (1000/T of 3). The motion represented by τ_{c1} and τ_{c2} may be attributed to methine and methylene protons, respectively, on the basis of the values of activation energy. An activation energy of the same order as the calculated value of τ_{c2} has been reported for the methylene group of amorphous polyethylene (3.72 kcal/mol) (30). $T_{1\rho}$ reflects the motion of methine groups at temperatures between 35°C and 10°C (1000/T of 3 and 3.5), but reflects the motion of methylene groups at

temperatures lower than 10°C. The observed $T_{1\rho}$ of methine groups diverges from the values calculated from τ_{c1} at temperatures above 35°C, indicating that the motion of methine groups has greater activation energy at temperature above 35°C. The temperature at which a break is observed in the temperature dependence is coincident with T_{mc}, described in the section of proton T_2.

Molecular Mobility as Determined by High-Resolution NMR

Laboratory and Rotating Frame Spin-Lattice Relaxation Times of Carbon

Figure 7 shows the typical spectra of freeze-dried γ-globulin formulation containing dextran, freeze-dried γ-globulin, and freeze-dried dextran, measured by high-resolution ^{13}C solid-state NMR (31). Peaks at 70 and 180 ppm are assigned to the dextran methine carbon and γ-globulin carbonyl carbon, respectively. The T_1 of each carbon, calculated from the signal decay, decreases with increasing temperature, indicating that relaxation occurs in the slow motional regime. The τ_c of dextran methine carbon then can be calculated from the observed T_1 according to equation (7), if the dipole-dipole interaction between carbon and proton is predominant in the relaxation process, and if the relaxation time can be expressed by a single τ_c.

$$\frac{1}{T_1} = \frac{1}{10}\gamma_C^2\gamma_H{}^2\left(\frac{h}{2\pi}\right)^2 r_{C-H}{}^{-6} \times \left[\frac{\tau_c}{1+(\omega_c-\omega_H)^2\tau_c{}^2} + \frac{3\tau_c}{1+\omega_c^2\tau_c{}^2} + \frac{6\tau_c}{1+(\omega_C+\omega_H)^2\tau_c{}^2}\right] \quad (7)$$

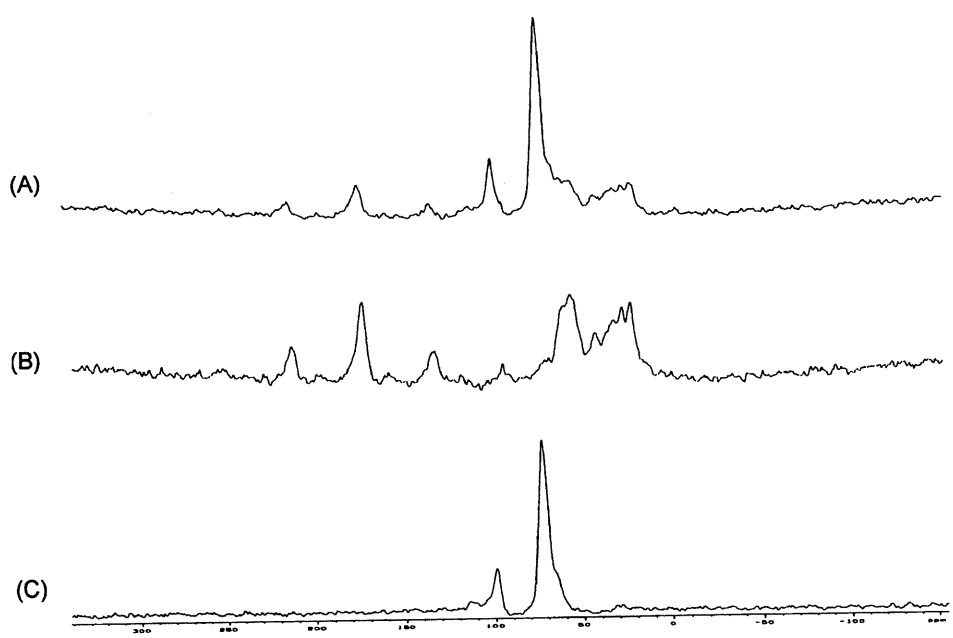

FIGURE 7 ^{13}C-NMR spectra of freeze-dried γ-globulin formulations containing dextran **(A)**, freeze-dried γ-globulin **(B)**, and freeze-dried dextran **(C)**.

where γ_C and γ_H are the gyromagnetic ratios of ^{13}C and ^{1}H, respectively, h is the Planck's constant, and ω_C and ω_H are the ^{13}C and ^{1}H resonance frequencies, respectively. $r_{C\text{-}H}$ is the C-H distance and a value of 1.2Å was used for the calculation.

In contrast, the τ_c of γ-globulin carbonyl carbon can be calculated from the observed T_1 using equation (8) if the relaxation due to chemical shift anisotropy is predominant, and if the relaxation time in the slow motional regime can be expressed by a single τ_c.

$$\frac{1}{T_1} = \frac{6}{40}\gamma_C{}^2 B_0^2 \delta_Z{}^2 \left(1 + \frac{\eta^2}{3}\right)\left(\frac{2\tau_c}{1+\omega_0{}^2\tau_c{}^2}\right) \tag{8}$$

where B_0, δ_Z, and η are the static field, the chemical shift anisotropy, and the asymmetric parameter, respectively. δ_Z and η are defined in terms of three principal components (δ_{11}, δ_{22}, and δ_{33}).

$$\begin{aligned}
&\delta_Z = \delta_{11} - \delta_0, \quad \eta = \frac{\delta_{22} - \delta_{33}}{\delta_{11} - \delta_0} \quad \text{when } |\delta_{11} - \delta_0| \geq |\delta_{33} - \delta_0| \\
&\delta_Z = \delta_{33} - \delta_0, \quad \eta = \frac{\delta_{22} - \delta_{11}}{\delta_{33} - \delta_0} \quad \text{when } |\delta_{11} - \delta_0| < |\delta_{33} - \delta_0| \\
&\text{where} \quad \delta_0 = \frac{\delta_{11} + \delta_{22} + \delta_{33}}{3}
\end{aligned} \tag{9}$$

Figure 8 shows the temperature dependence of τ_c determined for dextran methine carbon in freeze-dried dextran and freeze-dried γ-globulin/dextran formulation. For both systems, the τ_c of dextran methine carbon exhibits a significant change in the temperature dependence around the T_{mc} (35°C), the critical temperature of molecular mobility as determined by the spin-spin relaxation of proton. The greater decrease in the τ_c of dextran methine carbon at temperatures above the T_{mc} indicates that the motion of methine groups is significantly enhanced by increased global motion in addition to local segmental

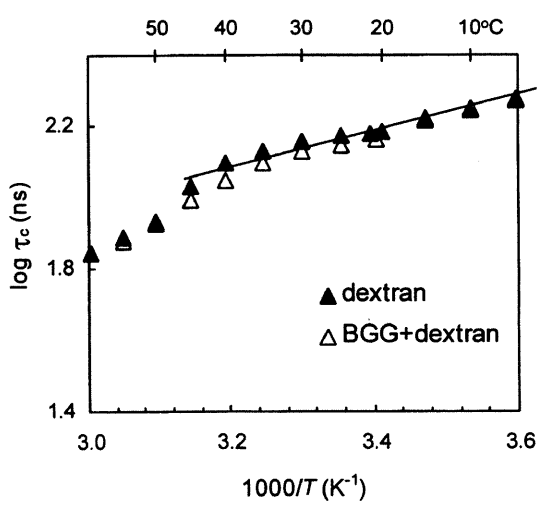

FIGURE 8 Temperature dependence of correlation time for dextran methine carbon in freeze-dried γ-globulin containing dextran 40 kDa.

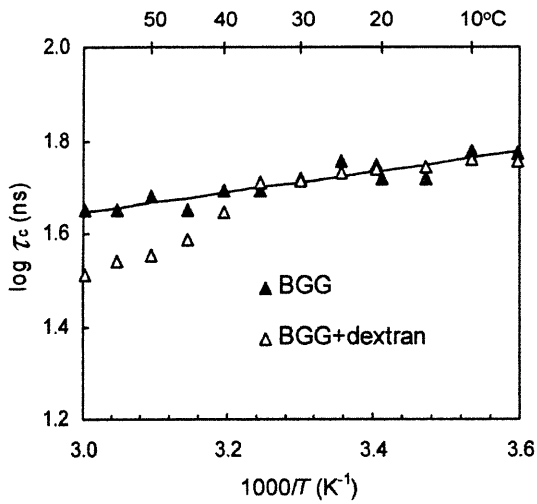

FIGURE 9 Temperature dependence of correlation time for γ-globulin carbonyl carbon in freeze-dried γ-globulin containing dextran 40 kDa.

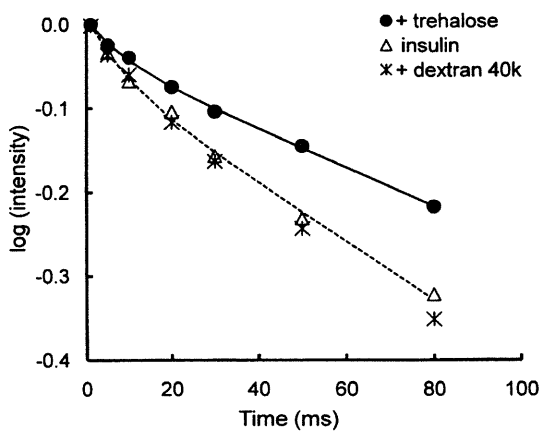

FIGURE 10 Time course of spin-lattice relaxation for insulin carbonyl carbon in freeze-dried insulin, insulin-dextran, and insulin-trehalose systems at 25°C and 12% RH.

motion. This interpretation is supported by the greater decrease in the τ_c of dextran methine proton at temperatures above the T_{mc}, as described in the previous section on proton $T_{1\rho}$ (Fig. 6).

The τ_c of the carbonyl carbon of freeze-dried γ-globulin exhibits linear Arrhenius-like temperature dependence as shown in Figure 9. In contrast, the τ_c of the carbonyl carbon of γ-globulin freeze-dried with dextran exhibits a change in the temperature dependence around 35°C, similar to that observed for the τ_c of dextran methine carbon. This indicates that at temperatures above T_{mc}, the molecular motion of γ-globulin is coupled with that of dextran, even though dextran is well known to cause phase separation with proteins.

Along with the T_1 of carbon, the $T_{1\rho}$ of carbon is useful as a measure of molecular mobility. Figure 10 shows the time courses of spin-lattice relaxation determined for the carbonyl carbon of insulin freeze-dried with dextran or trehalose, compared with that for insulin alone (32). Spin-lattice relaxation is not affected by dextran, but it is significantly retarded by trehalose. The $T_{1\rho}$ of

insulin carbonyl carbon in the insulin-trehalose system is longer than in the insulin-dextran system, indicating that the molecular mobility of insulin is decreased by trehalose, since longer $T_{1\rho}$ indicates slower motion in the slow motional regime (Fig. 3).

Retardation of spin-lattice relaxation of protein carbonyl carbon brought about by the addition of sugars is also observed for the carbonyl carbon of β-galactosidase freeze-dried with sucrose, trehalose, or stachyose, as shown in Figure 11 (33). The molecular mobility of the protein is most effectively decreased by sucrose.

The T_1 and $T_{1\rho}$ of protein carbonyl carbon described above represent the average of T_1 and $T_{1\rho}$ for multiple carbonyl carbons present in the protein molecule. More detailed site-specific analysis becomes possible by the ^{13}C-labeling of an amino acid at a specific site of interest.

Laboratory and Rotating Frame Spin-Lattice Relaxation Times of Fluorine

^{19}F-NMR has high sensitivity and specificity and has been used to determine the molecular mobility of ^{19}F-labeled proteins (34) as well as small molecules containing ^{19}F (35). Figure 12 shows the temperature dependence of T_1 and $T_{1\rho}$ of

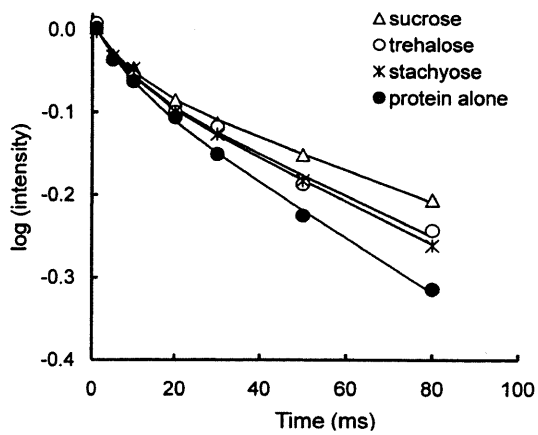

FIGURE 11 Time course of spin-lattice relaxation for carbonyl carbon of β-galactosidase freeze-dried with sucrose, trehalose, or stachyose at 25°C and 12% RH.

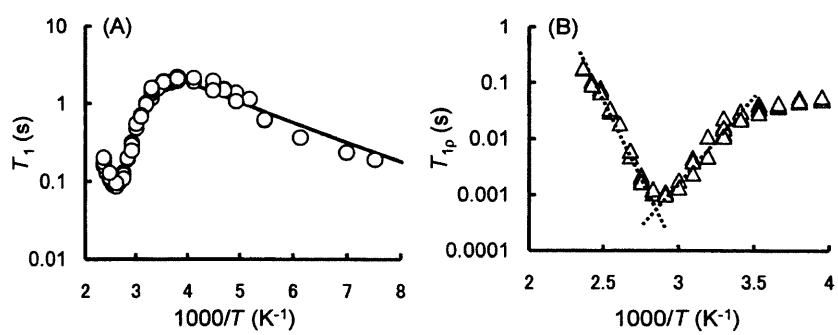

FIGURE 12 Temperature dependence of T_1 (**A**) and $T_{1\rho}$ (**B**) of flufenamic acid ^{19}F in solid dispersions with PVP. *Abbreviation*: PVP, polyvinylpyrrolidone.

^{19}F in amorphous flufenamic acid dispersed with PVP (drug-PVP, 7:3). The T_1 of ^{19}F shows a minimum at approximately 110°C as well as a maximum at approximately −10°C, as shown in Figure 12A. The temperature dependence can be described by assuming that the ^{19}F atom has two Arrhenius-type motions with an equivalent contribution to the process of T_1 but with different activation energies of 50 and 5 kJ/mol, as shown by the solid line in Figure 12A. The motion with greater activation energy may be attributed to β-relaxation and the other one to the rotation of the trifluoromethyl group, which is faster than β-relaxation.

The $T_{1\rho}$ of ^{19}F in flufenamic acid shows a minimum at approximately 60°C, as shown in Figure 12B. The temperature coefficient of $T_{1\rho}$ is about 50 kJ/mol at temperatures below 60°C, suggesting that $T_{1\rho}$ is determined by β-relaxation in this temperature range. In contrast, a greater temperature coefficient of $T_{1\rho}$ is observed at temperatures above 60°C, suggesting that $T_{1\rho}$ is determined by a larger-scale motion than β-relaxation. Thus, motion reflected by the T_1 and $T_{1\rho}$ of ^{19}F varies with temperature.

RELATIONSHIP BETWEEN STORAGE STABILITY AND MOLECULAR MOBILITY AS DETERMINED BY NMR RELAXATION TIMES

The storage stability of pharmaceuticals in the solid state is largely affected by molecular mobility. Changes in the molecular mobility of amorphous pharmaceuticals at T_g bring about changes in the temperature dependence of chemical and physical degradation rates. Coupling between chemical degradation and molecular mobility has been reported for several drugs of small molecular weight in freeze-dried formulation (1–5); hydrolysis of aspirin in freeze-dried hydroxypropyl-β-cyclodextrin/aspirin complex (1), hydrolysis of peptides in freeze-dried formulations containing cross-linked sucrose polymer (3), and deamidation of peptide in freeze-dried formulations containing poly(vinylpyrrolidone) (4,5). In addition to chemical instability, physical instability of pharmaceuticals, such as crystallization of amorphous compounds, is related to molecular mobility (36–40). Crystallization of freeze-dried sucrose is inhibited in the presence of PVP at a level as low as 10% due to the decreased molecular mobility of sucrose as indicated by the decreased enthalpy relaxation of the mixtures relative to sucrose alone (41).

Coupling between degradation and molecular mobility has also been reported for degradation of protein pharmaceuticals (6–15). An excellent correlation has been demonstrated between T_g and chemical degradation of freeze-dried antibody-vinca conjugate (8).

This section discusses the relationship between the storage stability of freeze-dried formulations and the molecular mobility as determined by NMR relaxation times, described in the previous section. Focus is placed on the degradation of small molecular weight drugs via bimolecular reaction and protein aggregation in the freeze-dried formulations.

Correlations Between Storage Stability and Structural Relaxation as Reflected by NMR Relaxation Times

NMR relaxation times are useful to determine fast dynamics of freeze-dried formulations, whereas structural relaxation of freeze-dried formulations, which

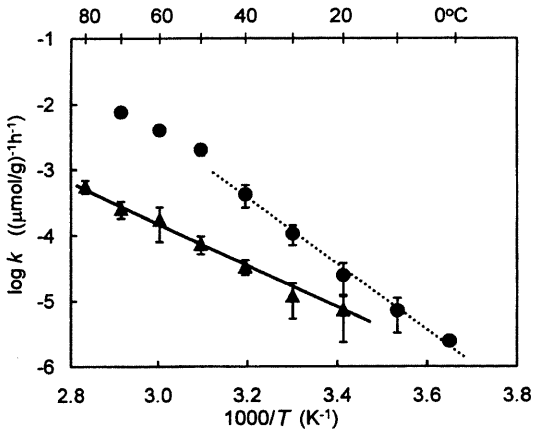

FIGURE 13 Temperature dependence of acetyl transfer between aspirin and sulfadiazine in freeze-dried formulations containing dextran at 12% (▲) and 60% RH (●).

is global mobility rapidly enhanced at temperatures above T_g, is also reflected by NMR relaxation times. Correlations between storage stability and structural relaxation as reflected by NMR relaxation times have been demonstrated for various freeze-dried formulations. Figure 13 shows the temperature dependence of the rate constant for acetyl transfer between aspirin and sulfadiazine in freeze-dried formulations containing dextran. Acetyl transfer is a bimolecular reaction in which the translational diffusion of reactant molecules becomes rate determining when molecular mobility is limited in the solid state (42). The rate constant of acetyl transfer (k_T) and the pseudo rate constant of hydrolysis ($k_{H,pseudo}$) that occurs in parallel with acetyl transfer in the presence of water are described by following equations.

$$\frac{d[SD]}{dt} = -k_T[SD][ASA] \tag{10}$$

$$\frac{d[ASA]}{dt} = -k_T[SD][ASA] - k_{H,pseudo}[ASA] \tag{11}$$

The temperature dependence of acetyl transfer at 60% RH exhibits a distinct break at approximately 40°C, although it is linear at 12% RH. The temperature of this distinct break observed at 60% RH is coincident with the T_{mc} as determined by the spin-spin relaxation measurements described in section "Molecular Mobility as Determined by NMR Relaxation Times." This indicates that the rate of acetyl transfer is affected by a change in the translational mobility of aspirin and sulfadiazine molecules at T_{mc}, resulting in a change in temperature dependence. The temperature dependence of acetyl transfer at 12% RH does not show any break because T_{mc} at 12% RH is higher than the highest temperature for the measurement. Compared with acetyl transfer, hydrolysis of aspirin occurring in parallel with acetyl transfer does not show such a distinct break at T_{mc}, even though hydrolysis is also a bimolecular reaction.

Similarly, no distinct break was observed in the temperature dependence of hydrolysis of cephalothin in freeze-dried formulations containing dextran, as shown in Figure 14. The hydrolysis rate of cephalothin increased with increasing humidity because the rate-limiting step involves water as a reactant. The

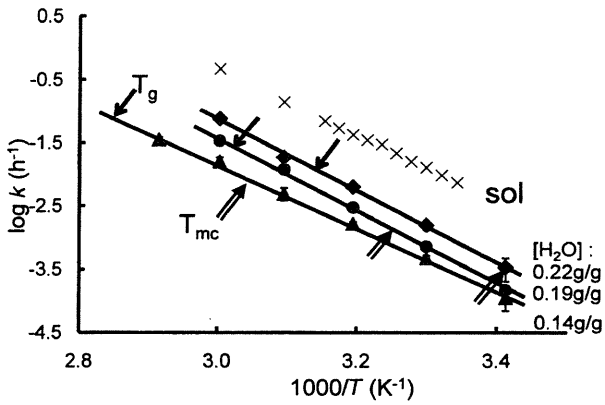

FIGURE 14 Temperature dependence of cephalothin hydrolysis in freeze-dried formulation containing dextran at 23% (▲), 60% (●), and 75% RH (◆).

temperature dependence of the apparent first-order rate constant is linear at all humidities in a manner similar to that of hydrolysis in aqueous solution, regardless of their T_{mc} indicated by arrows in the figure. The temperature dependence is also unaffected by the T_g of the formulations that are approximately 20°C higher than the T_{mc}. Since the translational mobility of drug and water molecules in freeze-dried formulations is affected by T_g and/or T_{mc}, the hydrolysis rate should be affected by T_g and/or T_{mc} if the translational diffusion of the drug and/or water molecules is rate limiting. The absence of a break in temperature dependence around T_g and T_{mc} suggests that the translational diffusion is not rate limiting. Since the translational diffusion of water can be considered to be much faster than that of the larger cephalothin molecule, the diffusion barrier of water molecules may be smaller than the chemical activational barrier. This interpretation is supported by the finding that the activation energy for the hydrolysis of cephalothin in the freeze-dried formulations containing dextran (between 23 and 26 kcal/mol) is close to the apparent activation energy obtained for hydrolysis in solution (24 kcal/mol). Because of the small diffusion barrier of water in freeze-dried formulations compared to the activational barrier, the hydrolysis rate of cephalothin is not affected by T_g and/or T_{mc}, even if the translational mobility of water molecules changes around T_g and/or T_{mc}.

Correlations Between Storage Stability and Fast Dynamics as Determined by NMR Relaxation Times

Protein aggregation, one of the most common degradation pathways of freeze-dried protein formulations, also appears to be closely related to the structural relaxation as reflected by NMR relaxation times. Figure 15 shows the temperature dependence of the time required for 10% protein aggregation (t_{90}) in freeze-dried β-galactosidase formulation containing methylcellulose (43). At 60% RH, the slope changes around the T_g measured by NMR (T_{mc}). No change in temperature dependence of t_{90} is observed at 12% RH, at which the T_{mc} is higher than the highest temperature for the measurement.

Apparent correlation between protein aggregation rate and structural relaxation is also observed for β-galactosidase freeze-dried with sugars. As shown in Figure 16, the slope of $t_{90} - T_g/T$ plots changes at around T_g, suggesting that aggregation rate is related to structural relaxation (33). However,

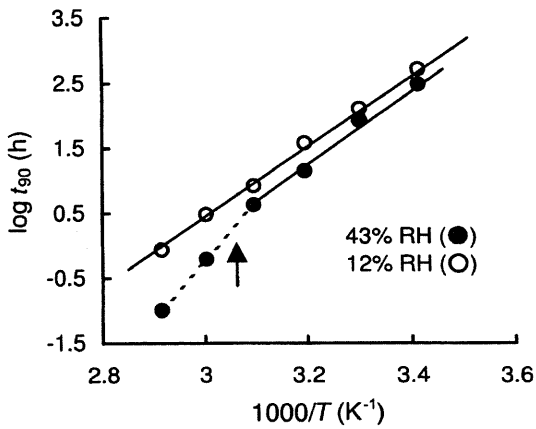

FIGURE 15 Temperature dependence of t_{90} for β-galactosidase aggregation in freeze-dried formulation containing methylcellulose.

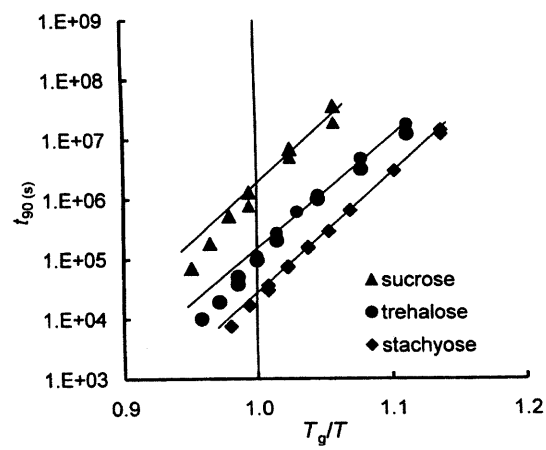

FIGURE 16 t_{90} for β-galactosidase aggregation in freeze-dried formulation containing sucrose, trehalose, or stachyose plotted against T_g/T.

structural relaxation cannot be considered to be the most relevant motion to the protein degradation, because sucrose, which has the shortest structural relaxation time, stabilizes the protein most effectively. These findings suggest that molecular motion other than structural relaxation contributes to the protein degradation. As shown in Figure 11, the $T_{1\rho}$ process of the protein carbonyl carbon is retarded by the addition of sugars, indicating that the fast dynamics of the protein is decreased by sugars. Sucrose is most effective in decreasing the protein dynamics. This suggests that the aggregation rate of β-galactosidase is correlated to the fast dynamics of the protein as determined by NMR relaxation times.

Figure 17 shows the temperature dependence of t_{90} observed for the degradation of insulin freeze-dried with trehalose or PVP (44). For insulin freeze-dried with trehalose stored at 12% RH, the slope of t_{90} – T_g/T plot changed at around T_g, suggesting that degradation rate of insulin is correlated with structural relaxation. In contrast, for insulin freeze-dried with PVP, t_{90} – T_g/T plots are linear at temperatures around T_g without a change in the slope. The value of t_{90} at T_g varies with humidity, indicating that structural relaxation is not the major factor that determines the degradation rate of insulin. If the

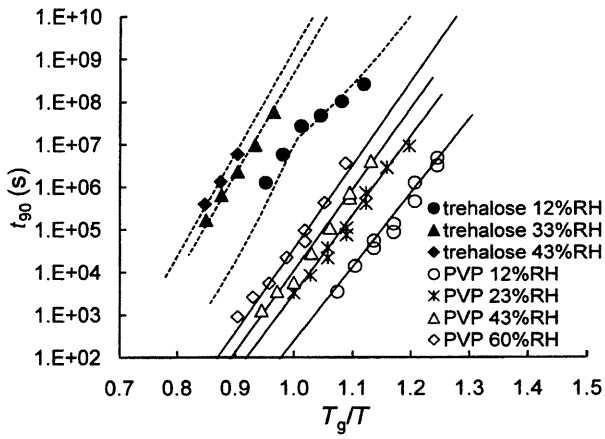

FIGURE 17 t_{90} for insulin degradation in freeze-dried formulation containing trehalose or PVP plotted against T_g/T.

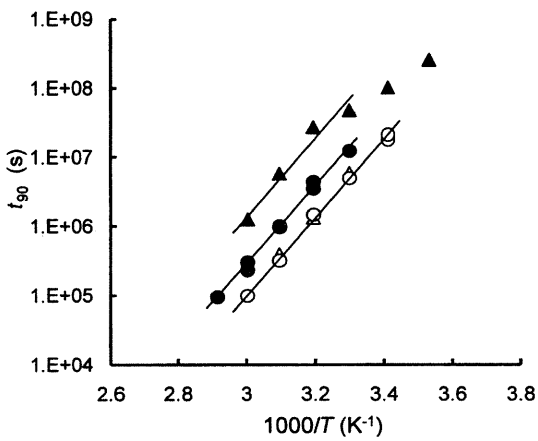

FIGURE 18 Temperature dependence of t_{90} for insulin degradation in freeze-dried formulation containing trehalose or dextran. ●, dextran 12% RH; ○, dextran 43% RH; ▲, trehalose 12% RH; △, trehalose 43% RH.

degradation rate is determined only by structural relaxation, t_{90} at T_g should not vary with humidity, because structural relaxation time is constant (100 seconds) at T_g regardless of humidity. These findings suggest that molecular motion other than structural relaxation contributes the insulin degradation, as suggested for the aggregation of β-galactosidase freeze-dried with sugars.

As shown in Figure 18, the t_{90} for the degradation of insulin freeze-dried with dextran is shorter than that of insulin freeze-dried with trehalose at 12% RH, and this difference in t_{90} is eliminated at 43% RH (32). As shown in Figure 10, the molecular mobility of the carbonyl carbon of insulin freeze-dried with trehalose, as determined by $T_{1\rho}$, is lower than that of insulin freeze-dried with dextran, as described in the section "Molecular Mobility as Determined by NMR Relaxation Times." This difference in mobility is eliminated at 43% RH, similar to the difference in t_{90}. These findings suggest that trehalose decreases the mobility of insulin in low humidity condition, and this decrease in mobility is related to the increase in insulin stability. Thus, the degradation rate of insulin also appears to be correlated to fast dynamics as determined by NMR relaxation times.

REFERENCES

1. Duddu SP, Weller K. Importance of glass transition temperature in accelerated stability testing of amorphous solids: case study using a lyophilized aspirin formulation. J Pharm Sci 1996; 85:345–347.
2. Herman BD, Sinclair BD, Milton N, et al. The effect of bulking agent on the solid-state stability of freeze-dried methylprednisolone sodium succinate. Pharm Res 1994; 11:1467–1473.
3. Streefland L, Auffret AD, Franks F. Bond cleavage reactions in solid aqueous carbohydrate solutions. Pharm Res 1998; 15:843–849.
4. Lai MC, Hageman MJ, Schowen RL, et al. Chemical stability of peptides in polymers. 1: Effect of water on peptide deamidation in poly(vinyl alcohol) and poly(vinyl pyrrolidone) matrixes. J Pharm Sci 1999; 88:1073–1080.
5. Lai MC, Hageman MJ, Schowen RL, et al. Chemical stability of peptides in polymers. 2. Discriminating between solvent and plasticizing effects of water on peptide deamidatin in poly(vinylpyrrolidone). J Pharm Sci 1999; 88:1081–1089.
6. Duddu SP, Zhang G, Dal Monte PR. The relationship between protein aggregation and molecular mobility below the glass transition temperature of lyophilized formulations containing a monoclonal antibody. Pharm Res 1997; 14:596–600.
7. Pikal MJ, Dellerman K, Roy ML. Formulation and stability of freeze-dried proteins: effects of moisture and oxygen on the stability of freeze-dried formulations of human growth hormone. Dev Biol Stand 1991; 74:21–38.
8. Roy ML, Pikal MJ, Rickard EC, et al. The effects of formulation and moisture on the stability of a freeze-dried monoclonal antibody-vinca conjugate: a test of the WLF glass transition theory. Dev Biol Stand 1991; 74:323–340.
9. Hageman M. Water sorption and solid-state stability of proteins. In: Ahern TJ, Manning MC, eds. Stability of Protein Pharmaceuticals. Part A: Chemical and Physical Pathways of Protein Degradation. New York: Plenum Press, 1992.
10. Bell LN, Hageman MJ, Muraoka LM. Thermally induced denaturation of lyophilized bovine somatotropin and lysozyme as impacted by moisture and excipients. J Pharm Sci 1995; 84:707–712.
11. Franks F. Freeze Drying: a combination of physics, chemistry, engineering and economics. Jpn J Freezing Drying 1992; 38:5–16.
12. Pikal M. Freeze-drying of proteins. BioPharm 1990; 3:26–30.
13. Prestrelski SJ, Pikal KA, Arakawa T. Optimization of lyophilization conditions for recombinant human interleukin-2 by dried-state conformational analysis using Fourier-transform infrared spectroscopy. Pharm Res 1995; 12:1250–1259.
14. Duddu SP, Dal Monte PR. Effect of glass transition temperature on the stability of lyophilized formulations containing a chimeric therapeutic monoclonal antibody. Pharm Res 1997; 14:591–595.
15. Costantino HR, Langer R, Klivanov AM. Aggregation of a lyophilized pharmaceutical protein, recombinant human albumin: effect of moisture and stabilization by excipients. Bio/Technology 1995; 13:493–496.
16. Kalichevsky MT, Jaroszkiewicz EM, Ablett S, et al. The glass transition of amylopectin measured by DSC, DMTA and NMR. Carbohydr Polym 1992; 18:77–88.
17. Kalichevsky MT, Jaroszkiewicz EM, Blanshard JMV. A study of the glass transition of amylopectin-sugar mixtures. Polymer 1993; 34:346–358.
18. Oksanen CA, Zografi G. Molecular mobility in mixtrures of absorbed water and solid poly(vinylpyrrolidone). Pharm Res 1993; 10:791–799.
19. Yoshioka S, Aso Y, Otsuka T, et al. Water mobility in poly(ethylene glycol)-, poly(vinylpyrrolidone)-, and gelatin-water systems as indicated by dielectric relaxation time, spin-lattice relaxation time, and water activity. J Pharm Sci 1995; 84:1072–1077.
20. Rubin CA, Wasylyk JM, Baust JG. Investigation of vitrification by nuclear magnetic resonance and differential scanning calorimetry in honey: a model carbohydrate system. J Agric Food Chem 1990; 38:1824–1827.
21. Shamblin SL, Tang X, Chang L, et al. Characterization of the time scales of molecular motion in pharmaceutically important glasses. J Phys Chem 1999; 103:4113–4121.

22. Andronis V, Zografi G. The molecular mobility of supercooled amorphous indomethacin as a function of temperature and relative humidity. Pharm Res 1998; 15:835–842.
23. Liu J, Rigsbee DR, StotzandM C, et al. Dynamics of pharmaceutical amorphous solid: the study of enthalpy relaxation by isothermal microcalorimetry. J Pharm Sci 2002; 91:1853–1862.
24. Hancock BC, Shamblin SL, Zografi G. Molecular mobility of amorphous pharmaceutical solids below their glass transition temperatures. Pharm Res 1995; 12:799–806.
25. Andronis V, Zografi G. Molecular mobility of supercooled amorphous indomethacin, determined by dynamic mechanical analysis. Pharm Res 1997; 14:410–414.
26. Yoshioka S, Aso Y, Kojima S. Dependence of the molecular mobility and protein stability of freeze-dried γ-globulin formulations on the molecular weight of dextran. Pharm Res 1997; 14:736–741.
27. Yoshioka S, Aso Y, Nakai Y, et al. Effect of high molecular mobility of poly(vinyl alcohol) on protein stability of lyophilized γ-globulin formulations. J Pharm Sci 1998; 87:147–151.
28. Yoshioka S, Aso Y, Kojima S. The effect of excipients on the molecular mobility of lyophilized formulations, as measured by glass transition temperature and NMR relaxation-based critical mobility temperature. Pharm Res 1999; 16:135–140.
29. Yoshioka S, Aso Y, Kojima S. Different molecular motions in lyophilized protein formulations as determined by laboratory and rotating frame spin-lattice relaxation times. J Pharm Sci 2002; 91:2203–2210.
30. Chen Q, Yamada T, Kurosu H, et al. Dynamic study of the noncrystalline phase of ^{13}C-laveled polyethylene by variable-temperature ^{13}C CP/MAS NMR spectroscopy. J Polym Sci B 1992; 30:591–601.
31. Yoshioka S, Aso Y, Kojima S, et al. Molecular mobility of protein in lyophilized formulations linked to the molecular mobility of polymer excipients, as determined by high resolution ^{13}C solid-state NMR. Pharm Res 1999; 16:1621–1625.
32. Yoshioka S, Miyazaki T, Aso Y. β-Relaxation of insulin molecule in lyophilized formulations containing trehalose or dextran as a determinant of chemical reactivity. Pharm Res 2006; 23:961–966.
33. Yoshioka S, Miyazaki T, Aso Y, et al. Significance of local mobility in aggregation of β-galactosidase lyophilized with trehalose, sucrose or stachyose. Pharm Res 2006; 23:961–966.
34. Afonin S, Glaser RW, Berditchevskaia M, et al. 4-Fluorophenylglycine as a label for ^{19}F NMR structure analysis of membrane-associated peptides. Chembiochem 2003; 4:1151–1163.
35. Aso Y, Yoshioka S, Miyazaki T, et al. Feasibility of ^{19}F-NMR for assessing the molecular mobility of flufenamic acid in solid dispersions. Chem Pharm Bull (Tokyo) 2009; 57:61–64.
36. Hancock BC, Zografi G. Characteristics and significance of the amorphous state in pharmaceutical systems. J Pharm Sci 1997; 86:1–12.
37. Andronis V, Zografi G. Crystal nucleation and growth of indomethacin polymorphs from the amorphous state. J Non-Cryst Solids 2000; 271:236–248.
38. Aso Y, Yoshioka S, Kojima S. Explanation of the crystallization rate of amorphous nifedipine and phenobarbital from their molecular mobility as measured by ^{13}C NMR relaxation time and the relaxation time obtained from the heating rate dependence of T_g. J Pharm Sci 2001; 89:128–143.
39. Aso Y, Yoshioka S, Kojima S. Molecular mobility-based estimation of the crystallization rates of amorphous nifedipine and phenobarbital in poly(vinylpyrrolidone) solid dispersions. J Pharm Sci 2004; 93:384–391.
40. Korhonen O, Bhugra C, Pikal MJ. Correlation between molecular mobility and crystallization growth of amorphous phenobarbital and phenobaribita with polyvinylpyrrolidone and L-proline. J Pharm Sci 2008; 97:3830–3841.
41. Shamblin SL, Zografi G. Enthalpy relaxation in binary amorphous mixtures containing sucrose. Pharm Res 1998; 15:1828–1834.